DTIC FILE COPY

(2)

SECURITY CLASSIFICATION OF THIS PAGE

REPORT DOCUMENTATION PAGE

AD-A221 829

1b. RESTRICTIVE MARKINGS: None

2b. DECLASSIFICATION/DOWNGRADING SCHEDULE

3. DISTRIBUTION/AVAILABILITY OF REPORT: Unlimited

4. PERFORMING ORGANIZATION REPORT NUMBER(S): interium technical report #37

5. MONITORING ORGANIZATION REPORT NUMBER(S)

6a. NAME OF PERFORMING ORGANIZATION: Department of Chemistry

6b. OFFICE SYMBOL (If applicable)

7a. NAME OF MONITORING ORGANIZATION: Office of Naval Research

6c. ADDRESS (City, State, and ZIP Code): Massachusetts Institute of Technology, 77 Mass. Avenue, Bldg. 6-335, Cambridge, MA 02139

7b. ADDRESS (City, State, and ZIP Code): Chemistry Division, 800 N. Quincy Street, Arlington, VA 22217

8a. NAME OF FUNDING/SPONSORING ORGANIZATION: Office of Naval Research

8b. OFFICE SYMBOL (If applicable)

9. PROCUREMENT INSTRUMENT IDENTIFICATION NUMBER: N00014-84-K-0553

8c. ADDRESS (City, State, and ZIP Code): Chemistry division, 800 N. Quincy Street, Arlington, VA 22217

10. SOURCE OF FUNDING NUMBERS

PROGRAM ELEMENT NO.	PROJECT NO.	TASK NO.	WORK UNIT ACCESSION NO.
		051-579	

11. TITLE (Include Security Classification): Electrochemical Behavior of the Oxide Formed by Reduction of RuO_4^{2-}...

12. PERSONAL AUTHOR(S): D.F. Lyons, M.O. Schloh, J.J. Hickman, and M.S. Wrighton

13a. TYPE OF REPORT: technical interim

13b. TIME COVERED: FROM 5/89 TO 5/90

14. DATE OF REPORT (Year, Month, Day): 5/16/90

15. PAGE COUNT: 47

16. SUPPLEMENTARY NOTATION: Prepared for publication in Chemistry of Materials

17. COSATI CODES

FIELD	GROUP	SUB-GROUP

18. SUBJECT TERMS (Continue on reverse if necessary and identify by block number): ruthenium oxide, microelectrochemical transistor

19. ABSTRACT (Continue on reverse if necessary and identify by block number)

See Attached Sheet

20. DISTRIBUTION/AVAILABILITY OF ABSTRACT: ☐ UNCLASSIFIED/UNLIMITED ☐ SAME AS RPT. ☐ DTIC USERS

21. ABSTRACT SECURITY CLASSIFICATION: Unlimited

22a. NAME OF RESPONSIBLE INDIVIDUAL: Mark S. Wrighton

22b. TELEPHONE (Include Area Code): 617-253-1597

22c. OFFICE SYMBOL

DD FORM 1473, 84 MAR — 83 APR edition may be used until exhausted. All other editions are obsolete.

SECURITY CLASSIFICATION OF THIS PAGE

90 05 24 109

ABSTRACT

Properties of macroscopic electrodes and arrays of closely spaced (1.2 μm) Au microelectrodes (~2 μm wide x 50 μm long x 0.1 μm high) coated with the oxide (RuO_x) derived from reduction of RuO_4^{2-} in 1 **M** NaOH are reported. XPS data show RuO_x consists of a mixture of Ru oxidation states with significant amounts of Ru^{IV}. RuO_x exhibits a well defined cyclic voltammetric wave centered at about 0.0 V vs. SSCE in pH 7.0 solution. The average of the anodic and cathodic peak current positions is taken to be $E^{0'}$ for the $Ru^{IV/III}$ couple. The position, shape and area of the wave at a given pH are insensitive to electrolyte composition for buffered solutions of LiCl, NaCl, $CaCl_2$, NH_4Cl, $NaClO_4$, Na(acetate), Na(tosylate), or Na(phosphate). A pH dependence of ~71 mV/pH unit from pH = 2 to pH = 14 is found for this wave. UV-vis spectroelectrochemistry shows four broad absorption bands in reduced RuO_x. Oxidation increases absorbance across the entire visible spectrum. Electrical connection of microelectrodes by RuO_x was verified by cyclic voltammetry. The steady state resistance of RuO_x films has been measured as a function of potential and was typically found to vary from ~10^9 ohms for the reduced film to ~10^6 ohms for the film at potentials ~100 mV positive of $E^{0'}$. At more positive potentials, film resistance increases. The minimum resistance corresponds to a resistivity of approximately 300 ohm-cm. The potential at which minimum resistance occurs has a 71 mV/pH unit dependence, but the

magnitude of the minimum resistance is not affected by pH. RuO_x-based microelectrochemical transistors can amplify power, but the maximum frequency (~0.1 Hz) is limited by the slow oxidation and reduction of RuO_x films. A pair of microelectrodes connected by RuO_x functions as a pH-sensitive microelectrochemical transistor and detection of a change of pH in a flowing stream was demonstrated. A model is proposed for the structure of RuO_x consisting of a relatively ordered lattice domain surrounded by oxoruthenium moieties.

Office of Naval Research

Contract NOOO14-84-K-0553

Task No. 051-597

Technical Report #37

Electrochemical Behavior of the Oxide Formed by Reduction of RuO_4^{2-}: A ph-Dependent Ruthenium Oxide-Based Microelectrochemical Transistor

by

Donald F. Lyons, Martin O. Schloh, James J. Hickman

and Mark S. Wrighton

Prepared for Publication

in

Chemistry of Materials

Massachusetts Institute of Technology
Department of Chemistry
Cambridge, MA 02139

[Prepared for publication as an article in

Chemistry of Materials]

Electrochemical Behavior of the Oxide Formed by Reduction of RuO_4^{2-}: A pH-Dependent Ruthenium Oxide-Based Microelectrochemical Transistor

Donald F. Lyons, Martin O. Schloh, James J. Hickman, and Mark S. Wrighton*

Department of Chemistry

Massachusetts Institute of Technology

Cambridge, Massachusetts 02139

* Address correspondence to this author.

ABSTRACT

Properties of macroscopic electrodes and arrays of closely spaced (1.2 μm) Au microelectrodes (~2 μm wide x 50 μm long x 0.1 μm high) coated with the oxide (RuO_x) derived from reduction of RuO_4^{2-} in 1 **M** NaOH are reported. XPS data show RuO_x consists of a mixture of Ru oxidation states with significant amounts of Ru^{IV}. RuO_x exhibits a well defined cyclic voltammetric wave centered at about 0.0 V vs. SSCE in pH 7.0 solution. The average of the anodic and cathodic peak current positions is taken to be $E^{0'}$ for the $Ru^{IV/III}$ couple. The position, shape and area of the wave at a given pH are insensitive to electrolyte composition for buffered solutions of LiCl, NaCl, $CaCl_2$, NH_4Cl, $NaClO_4$, Na(acetate), Na(tosylate), or Na(phosphate). A pH dependence of ~71 mV/pH unit from pH = 2 to pH = 14 is found for this wave. UV-vis spectroelectrochemistry shows four broad absorption bands in reduced RuO_x. Oxidation increases absorbance across the entire visible spectrum. Electrical connection of microelectrodes by RuO_x was verified by cyclic voltammetry. The steady state resistance of RuO_x films has been measured as a function of potential and was typically found to vary from ~10^9 ohms for the reduced film to ~10^6 ohms for the film at potentials ~100 mV positive of $E^{0'}$. At more positive potentials, film resistance increases. The minimum resistance corresponds to a resistivity of approximately 300 ohm-cm. The potential at which minimum resistance occurs has a 71 mV/pH unit dependence, but the

magnitude of the minimum resistance is not affected by pH. RuO_x-based microelectrochemical transistors can amplify power, but the maximum frequency (~0.1 Hz) is limited by the slow oxidation and reduction of RuO_x films. A pair of microelectrodes connected by RuO_x functions as a pH-sensitive microelectrochemical transistor and detection of a change of pH in a flowing stream was demonstrated. A model is proposed for the structure of RuO_x consisting of a relatively ordered lattice domain surrounded by oxoruthenium moieties.

We wish to report the characterization of an electrodeposited ruthenium oxide and its use as the device active material in a microelectrochemical transistor. In connection with microelectrochemical devices RuO_x is unique because it is useful over a wide pH range (2-14) and its "conductivity" vs. potential is similar to that of a conventional redox polymer showing a well-defined peak at a potential that depends on pH. Ruthenium oxides are currently of immense importance as electrocatalysts and have been studied extensively.[1] Ruthenium oxides formed by electrolysis of a solution species, however, have not been investigated in depth. Anderson and Warren described a route to an electrodeposited ruthenium oxide by oxidation of $(\eta^6\text{-}C_6H_6)Ru(OH_2)_3^{2+}$,[2] and Lam *et al.* reported the formation of a black precipitate upon reduction of RuO_4^{2-}.[3] We have examined the oxide formed upon reduction of RuO_4^{2-} in order to understand the behavior of ruthenium oxide-based microelectrochemical transistors. In particular, we report the potential dependence of conductivity and the pH dependence of the electrochemical response. Additionally, aspects of morphology, composition, and spectroelectrochemistry are reported. Throughout this paper, the oxide derived from reduction of RuO_4^{2-} will be referred to as RuO_x.

Closely spaced (1.2 μm) microelectrodes (~2 μm wide by ~50 μm long by ~0.1 μm high) are useful for studying the potential dependence of the conductivity of RuO_x.

Conductivity studies of $Ni(OH)_2$[4] and WO_3[5] films, as well as the organic conducting polymers polyaniline,[6] polypyrrole,[7] and poly(3-methylthiophene),[8] have been accomplished on such microelectrodes. Microelectrochemical transistors based on these materials have already been demonstrated.[4-8] It is important to note that materials with a conductivity that varies with electrochemical potential are necessary for the operation of microelectrochemical transistors. Materials that exhibit a constant conductivity at all potentials (for example, the oxide formed upon pyrolysis of $RuCl_3$)[9] cannot be used as the basis for such an electrochemical device. We will demonstrate that RuO_x does indeed exhibit a potential-dependent conductivity and that pH sensitive microelectrochemical transistors can be constructed with RuO_x.

Scheme I illustrates the operation of a microelectrochemical device based on RuO_x. A RuO_x film covers and electrically connects two adjacent microelectrodes. V_G, the gate voltage, establishes the state of charge of the RuO_x film. The current associated with the faradaic processes controlled by V_G is the gate current, I_G. A small potential difference, V_D, or the drain potential, can be maintained between the two microelectrodes. The more negative electrode is called the source and the more positive electrode the drain, by analogy to transistor nomenclature.[10] The current flowing between the microelectrodes is the drain current, I_D, and reflects

the conductivity of the RuO_x film for a particular V_G. When V_G equals V_G^1, where RuO_x is insulating, no current flows in the drain circuit: $I_D = 0$. When V_G is moved to a potential at which RuO_x is partially oxidized, V_G^2, the RuO_x is a better conductor and current flows in the drain circuit, $I_D > 0$, for a nonzero V_D. The maximum I_D obtained from a RuO_x-based device is at a V_G^2 which is near the peak potential of the cyclic voltammetry wave for the RuO_x. When V_G is moved to a potential at which RuO_x is fully oxidized, V_G^3, again $I_D > 0$, but I_D is found to be less than that obtained at V_G^2. Microelectrochemical transistors resemble solid-state transistors, but a key difference is that in a solid state device I_G is a capacitive current,[10] rather than a faradaic current associated with electrochemistry. A second significant difference for the RuO_x-based device is that the I_D-V_G characteristic shows a well-defined maximum at a V_G that depends on the pH of the medium to which the device is exposed.

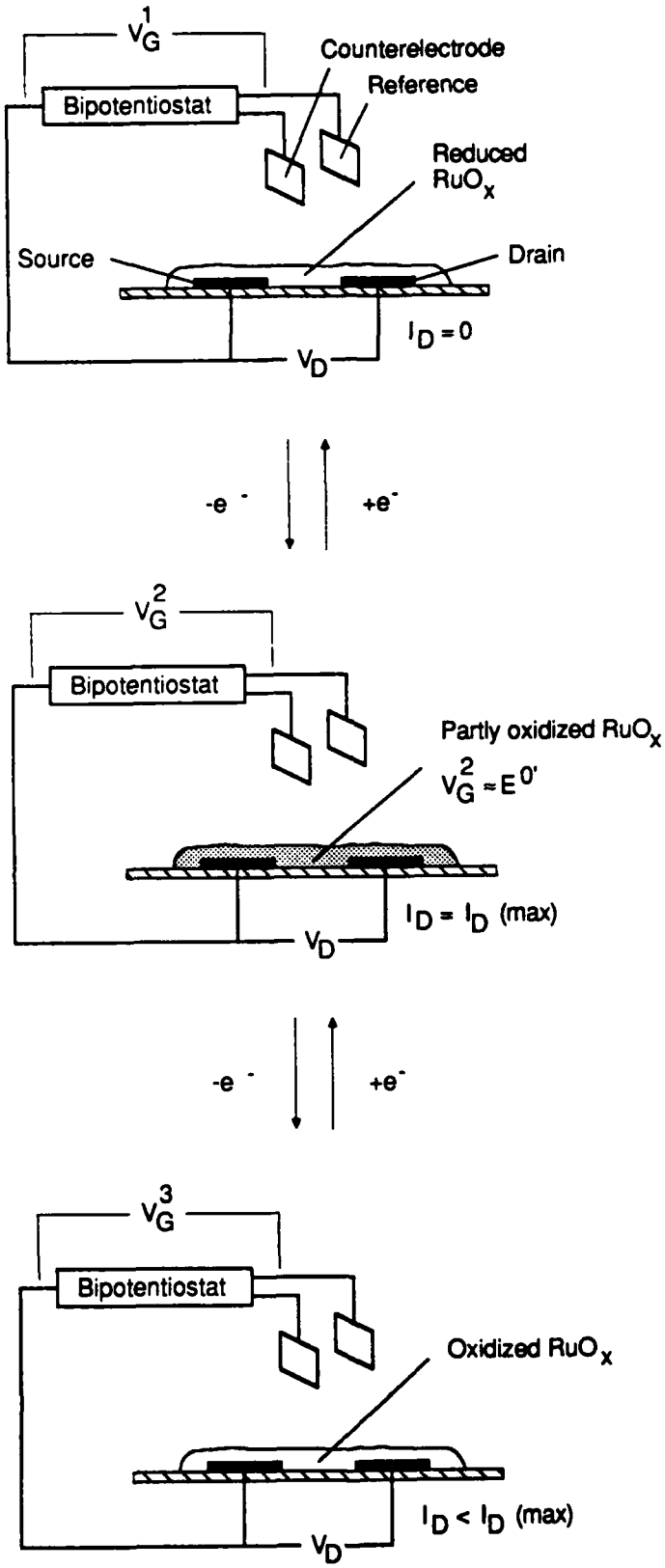

Scheme I. RuO_x-based microelectrochemical transistor.

EXPERIMENTAL SECTION

$K_2RuO_4 \cdot 2H_2O$ (Alfa) was used as received and stored in a controlled atmosphere chamber under N_2. All other chemicals as well as the SnO_2-coated glass were used as received from commercial sources.

Electrochemical instrumentation consisted of Pine Instruments RDE 4 Bipotentiostats with Kipp and Zonen BD 91 XYY'T recorders for microelectrode experiments, and an ECO 551 potentiostat controlled by a PAR 175 programmer with a Houston Instruments 2000 XY recorder for macroscopic electrode experiments. An SSCE (sodium chloride-saturated calomel electrode) was used as reference and all potentials quoted are vs. SSCE.

Spectroelectrochemistry was monitored on a Hewlett Packard 8451A rapid-scan spectrometer. Thickness measurements were made with a Tencor Instruments Alpha Step 100 surface profiler with a 12.5 μm radius stylus and a tracking force of 5 mg. Flowing streams were produced and delivered to microelectrodes using the pumps of a Hewlett Packard 1084-B liquid chromatograph. Scanning electron micrographs were obtained on a Hitachi S 800 instrument. Auger electron spectra were obtained on a Physical Electronics 660 Scanning Auger Microprobe. X-ray photoelectron spectra were obtained on a Physical Electronics 584 spectrometer or on a Surface Science Laboratories SSX-100 spectrometer and signals were referenced to C 1s at 284.6 eV.

Microelectrodes used in these experiments were of a design previously described.[4-8] Each chip consists of an array of eight parallel Au or Pt microelectrodes on an insulating layer of Si_3N_4, surrounded by macroscopic contact pads. Each microelectrode was 50 μm long, 2.4 μm wide, and 0.1 μm thick, and electrode separation was 1.2 μm. Insulation over all Au or Pt except for the microelectrodes and contact pads was either an additional layer of Si_3N_4 or epoxy. Cleaning and testing of microelectrodes followed previously published procedures.[6-8]

RuO_x deposition was done using a freshly prepared 5 m**M** K_2RuO_4/1 **M** NaOH solution. A two-compartment cell was used with the counter electrode separated from the working and reference electrodes. Cycling a macroscopic working electrode at 100 mV/s between -0.2 and -0.8 V led to the growth of a film of RuO_x associated with a cyclic voltammetry wave centered at -0.54 V. Gentle washing of the electrode after RuO_x deposition removed loosely bound particles, but did not affect the voltammetric signal. Deposition of RuO_x onto microelectrode arrays was performed in the same manner as on to macroscopic electrodes. Microelectrodes which were to be left underivatized were held at +0.1 V during the deposition procedure.

RESULTS

a. Microscopy, Auger Mapping, and Qualitative Aspects of Electrochemical Behavior of RuO_x. Deposition of RuO_x films is based on the literature procedure.[3] Electrode composition does not seem to be important, as we have successfully derivatized glassy carbon, SnO_2, Au, and Pt electrodes. Films of up to 0.5 μm thick have been prepared as measured by profilometry and SEM data. Films of this thickness are somewhat fragile and can be removed by vigorous washing, but 1000 Å thick films are extremely durable. Figure 1 shows a scanning electron micrograph of a RuO_x film deposited on Pt. The RuO_x appears granular and is also punctuated with larger holes which expose more oxide underneath. Unlike the oxide formed on Ru electrodes[11] or that formed by pyrolyzed $RuCl_3$,[9] both of which have a fairly compact morphology, RuO_x appears porous and nonuniform.

An Auger electron element map of a microelectrode array for which the central four electrodes had been derivatized and the other four electrodes were kept underivatized reveals that Ru is present on the central electrodes and absent on the outer electrodes, Figure 2. Interestingly, Ru signals were seen on the area surrounding the electrode array. This is consistent with a mechanism for RuO_x deposition in which RuO_4^{2-} is first reduced to a soluble Ru^{IV} species which subsequently decomposes to the insoluble RuO_x.[3] The small size of individual microelectrodes permits the soluble Ru^{IV} species to diffuse away and decompose on

electroinactive areas of the chip. The Auger map in Figure 2, however, establishes that it is possible to selectively modify the microelectrode array by controlling the potential of electrodes to remain free of RuO_x.

The cyclic voltammetry of the RuO_x film is depicted in Figure 3 and shows a wave centered at 0.0 V at pH 7. X-ray photoelectron spectroscopy (XPS) of RuO_x films has been used in an attempt to determine the Ru oxidation states of the RuO_x at different electrochemical potentials. An RuO_x film withdrawn from a pH 7.5 Na phosphate solution at -0.5 V shows a broad Ru $3d_{5/2}$ signal at 282.0 eV which indicates a mixture of Ru oxidation states.[12] The binding energy of RuO_x is very close to that reported for RuO_2[12b] indicating that Ru is present as at least the +4 oxidation state. Unfortunately, RuO_x-derivatized electrodes withdrawn from the pH 7.5 solution at 0.0 and 0.35 V give almost the same XPS Ru $3d_{5/2}$ peak as found for the sample withdrawn at -0.5 V results. It is possible that a degree of surface oxidation of RuO_x occurs when the reduced RuO_x is removed from solution and transferred to the XPS spectrometer, preventing clear distinction between the Ru $3d_{5/2}$ binding energies of the three RuO_x samples. The XPS results, therefore, do not better define the Ru oxidation states, and we adopt the earlier $Ru^{IV/III}$ assignment for the wave centered at ~0.0 V at pH = 7.[3] Further oxidation of RuO_x beyond the peak in the cyclic voltammetry, which begins at +0.35 V in pH 7.0 solution, is assigned to the $Ru^{VI/IV}$

couple.[3] At more positive potentials, the oxidation process overlaps H_2O oxidation to give O_2 evolution. Cycling RuO_x to the potential of O_2 evolution results in gradual film dissolution and loss of electroactivity. However, the film is remarkably durable as long as the electrode potential is not moved more than 0.2 V positive of the peak of the cyclic voltammetry wave. In one experiment a RuO_x-derivatized electrode was cycled for 18 h between +0.3 and -0.5 V in pH 7.5 solution with less than 5% loss in the area of the RuO_x voltammogram. At potentials negative of the $Ru^{IV/III}$ wave, the RuO_x film shows no faradaic activity until H_2 evolution occurs. H_2 oxidation current is not observed in the reverse sweep. A slight capacitive current is observed between the H_2 evolution and the $Ru^{IV/III}$ wave indicating that the film is not totally insulating in this potential regime (*vide infra*). Prolonged H_2 evolution does not affect the $Ru^{IV/III}$ voltammogram.

The voltammetry of the electrodeposited RuO_x film resembles that of the film produced upon oxidation of $(\eta^6\text{-}C_6H_6)Ru(OH_2)_3^{2+}$.[2] In contrast, ruthenium oxide films produced by pyrolysis of $RuCl_3$[9] or by Ru anodization[13-15] exhibit large capacitive currents with only small faradaic waves present. Ruthenium oxides formed by pyrolysis or anodization have electrochemical behavior[9,13-15] which resembles porous metallic electrodes with high conductivity and have very high surface area as deduced from the large double layer capacitance.[1,16] Apparently, RuO_x films

deposited from solution behave electrochemically in a manner similar to conventional redox polymers.[17] The integral of the cyclic voltammogram, coupled with measurements of RuO_x thickness, show that the oxidation/reduction associated with the wave at 0.0 V at pH = 7.0 involves >100 C/cm^3. This is similar to the charge density for conventional redox polymers.[17] It should be noted, though, that the electrodeposited RuO_x films described here are much better conductors (*vide infra*) than simple redox polymers such as those derived from viologens.[18]

Consistent with chemical changes in the RuO_x films upon oxidation and reduction, RuO_x exhibits electrochromism in the UV-vis region. Figure 4 shows spectroelectrochemistry of a RuO_x-coated SnO_2 electrode. The reduced RuO_x exhibits five absorption bands centered at 332, 374, 440, 548, 738 nm. Changing the electrode potential to more positive potentials increases absorbance across the entire spectrum. The actual UV-vis spectra appears to show no clearly defined new bands upon oxidation of the RuO_x film. However, the difference UV-vis does show broad new bands at 402, 454, 580 and 800 nm. Similar electrochromic behavior is found in solutions with a pH of 4.3 or 9.6.

b. pH and Electrolyte Dependence of Cyclic Voltammetry of RuO_x. RuO_x electrochemistry is pH dependent; the average of the anodic and cathodic peaks, $E^{0'}$, for $Ru^{IV/III}$ varies by 71 mV/pH unit from pH 2 to pH 14 as shown in Figure 5. In unbuffered solutions the voltammetric waves become poorly

defined. The pH dependence of $E^{0'}$ indicates that slightly more than one proton is lost from the film for every electron that is withdrawn (approximately 7 H^+ per 6 e^-). The pH dependence is similar for both NaCl and $NaNO_3$ supporting electrolytes. This type of non-Nernstian pH behavior has been observed in the voltammetry of several hydrous metal oxides (Ni,[19] Ir,[20] Rh,[21] Au,[22] Pd[23]) as well as in thermally prepared RuO_2.[24] This effect is usually attributed to the acid-base properties of the oxides. For example, proton loss from coordinated water molecules may occur upon oxidation due to the higher positive charge on the central metal atoms.[25]

We have studied cation and anion effects on the RuO_x electrochemistry. 0.05 **M** buffer/1.0 **M** electrolyte solutions were prepared. For cations, a pH 4.0 Na(acetate) buffer was used with LiCl, NaCl, $CaCl_2$, or NH_4Cl as the supporting electrolyte. For anions, a pH 7.0 Na(phosphate) buffer was used with NaCl, $NaClO_4$, or Na(tosylate) as supporting electrolyte. Additionally, a pH 7.5, 0.5 **M** Na(phosphate) solution was examined. No change in the shape, area, or position of the RuO_x voltammogram (5 mV/s) for a fixed pH was seen. These results indicate that, in general, RuO_x is insensitive to electrolyte composition as long as the solution pH is maintained by a buffer.

c. Scan Rate Dependence of Cyclic Voltammetry. The relationship of the voltammetric peak current to the scan rate is a widely used technique to determine the charge

transport properties of chemically modified electrodes.[17] A linear increase of peak current with increasing sweep rate is expected for very fast charge transport and a fall off from such a linear response signals kinetic sluggishness. We have examined the peak current vs. scan rate behavior of RuO_x-coated Pt electrodes. It is recognized that this method may be affected by uncompensated ohmic drop through the film, by the rate of electron exchange between the film and the electrode, or by localized pH changes at high scan rates.[26] The data, Figure 6, show qualitatively better charge transport through RuO_x at low pH's. At low scan rates no pH effect is observed on peak current, but the higher scan rates reveal slow oxidation in basic solutions. AC impedance results on anodically and thermally grown ruthenium oxides were interpreted as showing proton motion to be important in the conduction mechanism,[27] but this does not provide insight into why low pH results in faster oxidation. The RuO_x film thickness may slightly shrink under acidic conditions due either to neutralization of anionic moieties in the film or formation of hydrogen bonds between oxyruthenium centers.

We have also characterized the cyclic voltammetry of RuO_x on microelectrode arrays. RuO_x is deposited on the arrays by the same procedure used for macroscopic electrodes. The cyclic voltammetry of four adjacent Au microelectrodes derivatized with RuO_x is shown in Figure 7. At 20 mV/s sweep rate the area of the cyclic voltammogram of

all four electrodes driven together is essentially the same as that of the individual electrodes. This indicates that there is an electrical connection between the microelectrodes via RuO_x such that at 20 mV/s nearly all of the RuO_x is electrically accessible from any one of the four derivatized microelectrodes. If there were no connection, the area of the cyclic voltammogram of the four microelectrodes driven together would be the sum of the individual voltammograms. The cyclic voltammograms at 50 mV/s in Figure 7 do show that not all the RuO_x is accessible by addressing any one electrode. The difference between the data for the 20 and 50 mV/s sweep rate is due to the relatively sluggish charge transport in the RuO_x. At very slow scan rates, <10 mV/s, all RuO_x accessible to one microelectrode is accessible to another RuO_x-connected microelectrode. Similar behavior has been reported for WO_3- and $Ni(OH)_2$-derivatized microelectrode arrays.[4,5]

d. Potential Dependence of the RuO_x Resistance. An important property of RuO_x is its resistance as a function of its electrochemical potential. This property can be measured using two microelectrodes connected by a RuO_x film. Like previously characterized microelectrochemical devices, the change in resistance of RuO_x is associated with the injection or withdrawal of charge through an electrochemical redox process. Measurement of the resistance entails bringing adjacent, RuO_x-connected electrodes to a given potential, V_G, waiting until redox equilibrium is

established, and slowly scanning the potential of one microelectrode by a small amount around V_G, while holding the adjacent electrode at V_G. With RuO_x-connected microelectrodes, measurements were made ~5 minutes after moving to a new V_G. Changes in resistance are observed by varying V_G through the region where redox processes occur. The current passing between the electrodes was measured and related to the resistance by Ohm's law.

The data in Figure 8 show that the resistance of RuO_x-connected microelectrodes varies by about three orders of magnitude, from ~10^9 ohms to ~10^6 ohms, as V_G is varied from -0.4 to 0.1 V, in pH 7.5 solution. At more positive potentials, film resistance actually increases by an order of magnitude. A similar resistance minimum has been observed for polyaniline-[6] and poly(3-methylthiophene)-[8b] connected microelectrodes. Such behavior is expected for conventional redox polymer-based microelectrochemical transistors.[28] The resistance minimum seen for RuO_x-connected microelectrodes is pH-dependent, and occurs ~100 mV positive of the peak in the cyclic voltammogram for RuO_x at a given pH. The measured resistance of different samples of RuO_x may vary from the data in Figure 8 by up to an order of magnitude, but the change in resistance for a particular sample never varies by more than three orders of magnitude. The minimum resistance of RuO_x-connected microelectrodes is much higher than for polyaniline, polypyrole, or poly(3-methylthiophene) derivatized onto microelectrodes.[6-8] In

the insulating state the resistance, as for WO_3[5] and $Ni(OH)_2$[4], is lower than for the conducting organic polymers. The point is that the RuO_x shows only a ~1000-fold change in conductivity and is always moderately conducting. The low resistance for RuO_x in the "insulating" state gives rise to the small charging currents observed negative of the peak in the cyclic voltammetry.

The resistance of RuO_x-connected microelectrodes *per se* is not especially meaningful information, as it can only be referenced to the resistance of other redox-active electronic conductors derivatized on closely spaced microelectrodes of the same geometry. Unlike the resistance, the resistivity, ρ, defined in equation (**1**), is a characteristic property of a material.

$$R = \rho\ (l/A) \qquad (1)$$

In equation (**1**), l is the length of a uniform conductor, and A is its cross sectional area. Assuming complete uniformity of RuO_x films, an approximate calculation of the resistivity can be made using the well-defined microelectrode geometry. For typical RuO_x-based devices, the 50 μm long microelectrodes are covered with a 0.5-1.0 μm thick film. The length is taken to be the 1.2 μm spacing between microelectrodes. Calculations indicate that in the maximum conducting state, the resistivity of electrochemically deposited RuO_x is 200-400 Ω-cm. This value is about equal

to the resistivity of moderately doped single crystal semiconductors,[10] but much larger than conventional redox polymers such as polyviologens.[18] The sample to sample variability in resistance is probably a result of differences in RuO_x film thickness rather than in resistivity. While the resistivity of RuO_x may be high for a "conducting" material, it is the potential dependence of the resistivity that leads to interesting consequences in connection with microelectrochemical transistors.

e. Transistor Properties of RuO_x-Connected Microelectrode Arrays. It has been established that redox materials that undergo large changes in resistance upon redox cycling can be used in transistor-like devices as the active switching material.[4-8] We have characterized the transistor properties of RuO_x-based microelectrochemical transistors. As expected from the relatively high resistance of the conducting state, the response times and amplification properties of devices based on the RuO_x films are not as good as those of devices based on materials such as poly(3-methylthiophene) and polyaniline which can amplify power at frequencies approaching 100 kHz.[29] However, RuO_x is durable over a wider pH range than other materials used to prepare pH-sensitive microelectrochemical transistors.

Based on the resistance data in Figure 8 and the configuration represented in Scheme I, when V_G is moved from V_G^1, where RuO_x is reduced, to V_G^2, where RuO_x is partially oxidized, and there is a potential difference V_D between two

adjacent microelectrodes, I_D can be expected to go from close to zero to a finite value that depends on the magnitude of V_D. Figure 9 shows I_D vs. time for a RuO_x-based transistor where V_G is stepped from -0.50 to +0.05 V and back in a pH 7.5 solution. With V_D = 100 mV, I_D shifts reproducibly from zero at V_G = -0.50 V to 140 nA at V_G = 0.1 V. The limiting I_D for the 100 mV V_D implies a resistance of approximately $7.1 \times 10^5\ \Omega$ at V_G = 0.1 V. The device takes approximately 10 s to achieve a steady state I_D. The current spikes upon scan reversal are indicative of the charging (or gate) current, I_G, necessary to turn the device on and off. While the magnitude of I_D is limited at fixed V_D by the RuO_x resistance (and therefore V_G), the rate at which a particular I_D is attained is limited by the rate of faradaic processes associated with switching the RuO_x between different states of charge.

Evidence that RuO_x-based microelectrochemical transistors function as electrical power amplifiers is illustrated in Figure 10, which shows the magnitudes and relationships of V_G, I_G, and I_D, for a slow triangular V_G variation between -0.35 and +0.05 V in pH 7.0 buffer. The average power amplification, $\underline{A}$, is given by equation (2).

$$\underline{A} = \frac{\text{average power in the drain circuit}}{\text{average power in the gate circuit}} \qquad (2)$$

For the data shown in Figure 11, A is equal to 1.8. In theory, at the same frequency and surface coverage, differences in the amplification ability of microelectrochemical transistors depend on the maximum conductivity of the materials used to connect adjacent microelectrodes. We find the observed amplification properties for devices prepared from redox active metal oxides and the conducting polymers accurately reflect the relative maximum conductivities of the materials. Power amplification is intrinsically frequency dependent in that I_G increases with scan rate. Furthermore, at sufficiently high frequencies, limitations in rates of faradaic processes preclude complete turn on/turn off. The data in Figure 10 are obtained in the mHz frequency domain, while polyaniline-based microelectrochemical transistors with similar electrode geometry can amplify power at frequencies approaching 1 kHz.[29a] The slow operating speed of RuO_x-based microelectrochemical transistors is limited by the slow electrochemistry of the RuO_x films. At frequencies higher than ~1 Hz, the RuO_x-based transistors do not amplify power, i.e. $A < 1$.

Figure 11 illustrates the steady state current voltage characteristics of a RuO_x-based microelectrochemical transistor. V_D is fixed at 100 mV and V_G is slowly scanned across the potential regime of interest. This RuO_x transistor was examined in three solutions of differing pH. We find essentially no difference in the maximum obtainable

I_D from pH to pH. The potential at which I_D is a maximum occurs ~100 mV positive of the peak of the cyclic voltammogram in the same electrolyte and shifts by 71 mV/pH unit. Since I_D depends on the charge transport properties of RuO_x, these steady state data agree with the cyclic voltammetry results, at slow scan rates, on macroscopic electrodes.

The pH-dependent nature of the I_D-V_G curves serves as the basis for a pH sensor, Figure 12. A RuO_x transistor was placed in the effluent stream of an HPLC and the pH of the stream varied from 5.5 to 7.3. V_G was fixed at 0.0 V and V_D was set at 100 mV. At this V_G, RuO_x is poorly conducting in pH 5.5 solution, but is much more conducting in pH 7.3 solution. Accordingly, I_D for this device is high in pH 7.3 and low in pH 5.5. The RuO_x-based device is durable and maintains nearly constant I_D values over five hours of operation. The use of a RuO_x-based transistor is constrained at a fixed V_G by H_2 evolution at lower pH's and by the degradation at potentials ~0.2 V more positive of the peak of the cyclic voltammetry wave. However, the stability of RuO_x over a wide pH range is a considerable improvement over WO_3- and $Ni(OH)_2$-based transistors[4,5] which fail in basic and acidic media respectively.

DISCUSSION

ruthenium tetra oxide ion

Reduction of RuO_4^{2-} in alkaline solution results in deposition of an oxide, RuO_x, exhibiting characteristics intermediate between "redox conducting" and "electronically

conducting" materials. Like a conventional redox polymer, RuO_x shows a well-defined cyclic voltammetry wave and a conductivity maximum at a potential close to the peak of the wave.[28] However, conductivity values obtained for RuO_x are much closer to those obtained for electronically conducting polymers and metal oxides. The $E^{0'}$ of RuO_x is pH-sensitive, 71 mV/pH unit in the pH range of 2-14. These properties allow the demonstration of a RuO_x-based pH sensitive microelectrochemical transistor having a pH-dependent I_D maximum in a I_D vs. V_G plot and which is durable over a wide pH range (2-14). Additionally, the redox properties of the RuO_x allow the demonstration of a pH-dependent microelectrochemical diode.[30]

We believe that the electrochromism, voltammetry, conducting maximum, and the large "background" conductivity of RuO_x can be explained by the following model. As depicted in Figure 13, the structure of RuO_x may consist of domains of a relatively ordered ruthenium-oxygen lattice surrounded by electroinactive oxoruthenium moieties. The UV-Vis absorption spectrum of RuO_x is a combination of absorption bands that are essentially unaffected by the state of charge of the RuO_x from the oxoruthenium moieties, and bands that grow in upon oxidation of the ruthenium-oxygen networks. The redox process in RuO_x probably involves gain and loss of either protons or hydroxide groups fron the ruthenium-oxygen network. It follows that while the electrolyte must be buffered to observe a well-defined

RuO_x voltammetric wave, the particular electrolyte composition has no effect on this wave. In addition, the absence of specific electrolyte effects on RuO_x voltammetry suggests that the electroactive networks are open and porous. Such porous structures have been postulated for other hydrous metal oxides.[25] The magnitude of the resistivity of RuO_x implies some degree of electron delocalization and the existence of an electronic band. As RuO_x is oxidized or reduced this band is emptied of or filled with, electrons, and the partially filled band exhibits the highest conductivity. The heterogeneous structure of RuO_x limits the maximum conductivity by limiting electron mobility, but also introduces enough localized states, which can accept or donate electrons, to give a residual conductivity even when RuO_x is fully reduced.

Acknowledgements. We thank the Office of Naval Research and Defense Advanced Research Projects Agency for partial support of this research. We also acknowledge support from the National Science Foundation Materials Research Laboratory at M.I.T.

REFERENCES

1. Trasatti, S.; O'Grady, W. E. In *Advances in Electrochemistry and Electrochemical Engineering*; Gerischer, H., and Tobias, C. W., Eds.; Wiley: New York, **1981**; Vol. 12, p 177.
2. Anderson, D. P.; Warren, L. F. *J. Electrochem. Soc.* **1984**, *131*, 347.
3. Lam, K. W.; Johnson, K. E.; Lee, D. G. *J. Electrochem. Soc.* **1978**, *125*, 1069.
4. Natan, M. J.; Bélanger, D.; Carpenter, M. K.; Wrighton. M. S. *J. Phys. Chem.* **1987**, *91*, 1834.
5. Natan, M. J.; Mallouk, T. E.; Wrighton, M. S. *J. Phys. Chem.* **1987**, *91*, 648.
6. Paul, E. W.; Ricco, A. J.; Wrighton, M. S. *J. Phys. Chem.* **1985**, *89*, 1441.
7. Kittlesen, G. P.; White, H. S.; Wrighton, M. S. *J. Amer. Chem. Soc.* **1984**, *106*, 7389.
8. (a) Thackeray, J. T.; White, H. S.; Wrighton, M. S. *J. Phys. Chem.* **1985**, *89*, 5133; (b) Ofer, D.; Wrighton, M. S. *J. Amer. Soc.* **1988**, *110*, 4467.
9. (a) Galizzioli, D.; Tantardini, F. Transatti, S. *J. Appl. Electrochem.* **1975**, *5*, 203; (b) Pizzini, S.; Buzzana, G.; Mari, C.; Rossi, K.; Torcho, S. *Mat. Res. Bull.* **1972**, *7*, 449
10. Sze, S. M. *Physics of Semiconductor Devices, 2nd Edition*; Wiley-Interscience: New York, **1981**.
11. Birss, V.; Myers, R.; Angerstein-Kozlowska, H.; Conway,

B. E. *J. Electrochem. Soc.* **1984**, *131*, 1502.

12. (a) Kim, K.S.; Winograd, N. *J. Catal.* **1974**, *35*, 66; (b) Folkesson, B. *Acta Chem. Scand.* **1973**, *27*, 287.

13. (a) Trasatti, S.; Buzzanca, G. *J. Electroanal. Chem.* **1971**, *29*, App. 1. (b) Galizzioli, D.; Tantardini, F.; Trasatti, S. *J. Appl. Electrochem.* **1974**, *4*, 57.

14. Hadzi-Jordanov,S.; Angerstein-Kozlowska, H.; Vukovic, M.; Conway, B. E. *J. Electrochem. Soc.* **1978**, *125*, 1473.

15. Burke, L. D.; Mulcahy, J. K.; Venkatesan, S. *J. Electroanal. Chem.* **1977**, *81*, 339.

16. Feldberg, S. W. *J. Amer. Chem. Soc.* **1984**, *106*, 4671.

17. Murray, R.W. in *Electroanalytical Chemistry, Vol. 13;* Bard, A.J., (Ed), Marcel Dekker; New York, **1984**, p. 191.

18. Lewis, T. J.; White, H. S.; Wrighton, M. S. *J. Amer. Chem. Soc.* **1984**, *106*, 6947.

19. Burke, L. D.; Twomey, T. A. M. *J. Electroanal. Chem.* **1984**, *162*, 101.

20. Burke, L. D.; Whelan, D. P. *J. Electroanal. Chem.* **1984**, *162*, 121.

21. Burke, L. D.; O'Sullivan, E. J. M. *J. Electroanal. Chem.* **1981**, *129*, 133.

22. Burke, L. D.; Lyons, M. E.; Whelan, D. P. *J. Electroanal. Chem.* **1982**, *139*, 131.

23. El Wakkad, S. E. S.; Shams El Din, A. M. *J. Chem. Soc.* **1954**, 3094.

24. Burke, L. D.; Healy, J. F. *J. Electroanal. Chem.* **1981**,

124, 327.

25. Burke, L. D.; Lyons, M. E. G. In *Modern Aspects of Electrochemistry, No. 18;* White, R. E., Bockris, J. O'M., Conway, B. E., Eds.; Plenum: New York, **1986;** p 169.

26. Laviron, E. In *Electroanalytical Chemistry, Vol. 12;* Bard, A. J., Ed.; Marcel Dekker: New York, **1982;** p 53.

27. Rishpon, J.; Gottesfeld, S. *J. Electrochem. Soc.* **1984**, *131*, 1960.

28. (a) Belanger, D.; Wrighton, M.S. *Anal. Chem.*, **1987**, *59*, 1426; (b) Shu, S. F.; Wrighton, M. S. *J. Phys. Chem.* **1988**, *92*, 5221; (c) Shu, S. F.; Wrighton, M. S. *ACS Symposium Series*, No. 378; Soriaga, M. P., Ed.; ACS, Washington, **1988**.

29. Lofton, E. P.; Thackeray, J. W.; Wrighton, M. S. *J. Phys. Chem.* **1986**, *90*, 6080; (b) Jones, E. T. T.; Chyan, O. M.; Wrighton, M. S. *J. Am. Chem. Soc.* **1987**, *109*, 5526.

30. Schloh, M. O.; Wrighton, M. S. *Chemistry of Materials*, submitted (following article in this issue).

FIGURE CAPTIONS

Figure 1. Scanning electron micrograph of RuO_x deposited onto a Pt electrode.

Figure 2 Scanning Auger element map of Ru (top) and scanning electron micrograph (bottom) of a microelectrode array in which the central four electrodes are derivatized witk RuO_x and the other four electrodes kept underivatized

Figure 3. Cyclic voltammetry of glassy carbon/RuO_x in pH 7, 0.05 **M** Na(phosphate)/0.3 **M** $NaNO_3$ solution. Scan rate: 10 mV/s.

Figure 4. UV-vis absorption (top) and difference absorption (bottom) spectra for SnO_2/RuO_x electrode potentiostatted at -0.6, -0.5, -0.4, -0.3, -0.2, -0.1, 0.0, 0.1, 0.2, 0.3, and 0.35 V vs. SSCE. The RuO_x film thickness is ~1300 Å.

Figure 5. Half wave potential of RuO_x as a function of pH. ●: C/RuO_x; ▲: Pt/RuO_x (both in 0.05 **M** buffer/1.0 **M** NaCl). ×: Pt/RuO_x in 0.05 **M** buffer/1.0 **M** $NaNO_3$. Extrapolation of this line gives $E^{0'}$ = +0.50 V vs. SSCE at pH = 0.

Figure 6. Peak anodic current for the RuO_x voltammetric wave at a Pt/RuO_x electrode. Soltions are 0.05 **M** buffer/1.0 **M** $NaNO_3$.

Figure 7. Cyclic voltammograms at pH 7.5 of the four individual adjacent RuO_x-connected microelectrodes and of the four microelectrodes driven together.

Figure 8. Resistance of RuO_x-connected microelectrodes as a function of V_G at pH 7.5. The data was obtained by scanning one electrode +-25 mV about V_G at 50 mV/s. The resistance is plotted on a logarithmic scale.

Figure 9. I_D vs. time for a RuO_x-based transistor at pH 7.5 as V_G is stepped repetitively every 20 s from -0.50 to +0.05 V vs. SSCE and back. V_D = 100 mV.

Figure 10. Simultaneous measurement and phase relationship of V_G, I_G, and I_D for a RuO_x-based microelectrochemical transistor at pH 7.0 as V_G is repetitively swept linearly from -0.35 to +0.05 V vs. SSCE and backat a frequency of 0.1 Hz. V_D = 100 mV.

Figure 11. pH dependence of steady state I_D vs V_G (at fixed V_D = 100 mV) for a RuO_x-based microelectrochemical transistor.

Figure 12. I_D vs. time for a RuO_x-based microelectrochemical transistor as the pH of a continuously

flowing stream is varied from 5.5 to 7.3. V_G = 0.0 V vs. SSCE and V_D =100 mV.

Figure 13. Proposed structure of RuO_x. Oxoruthenium moieties surround a porous ruthenium-oxygen lattice.

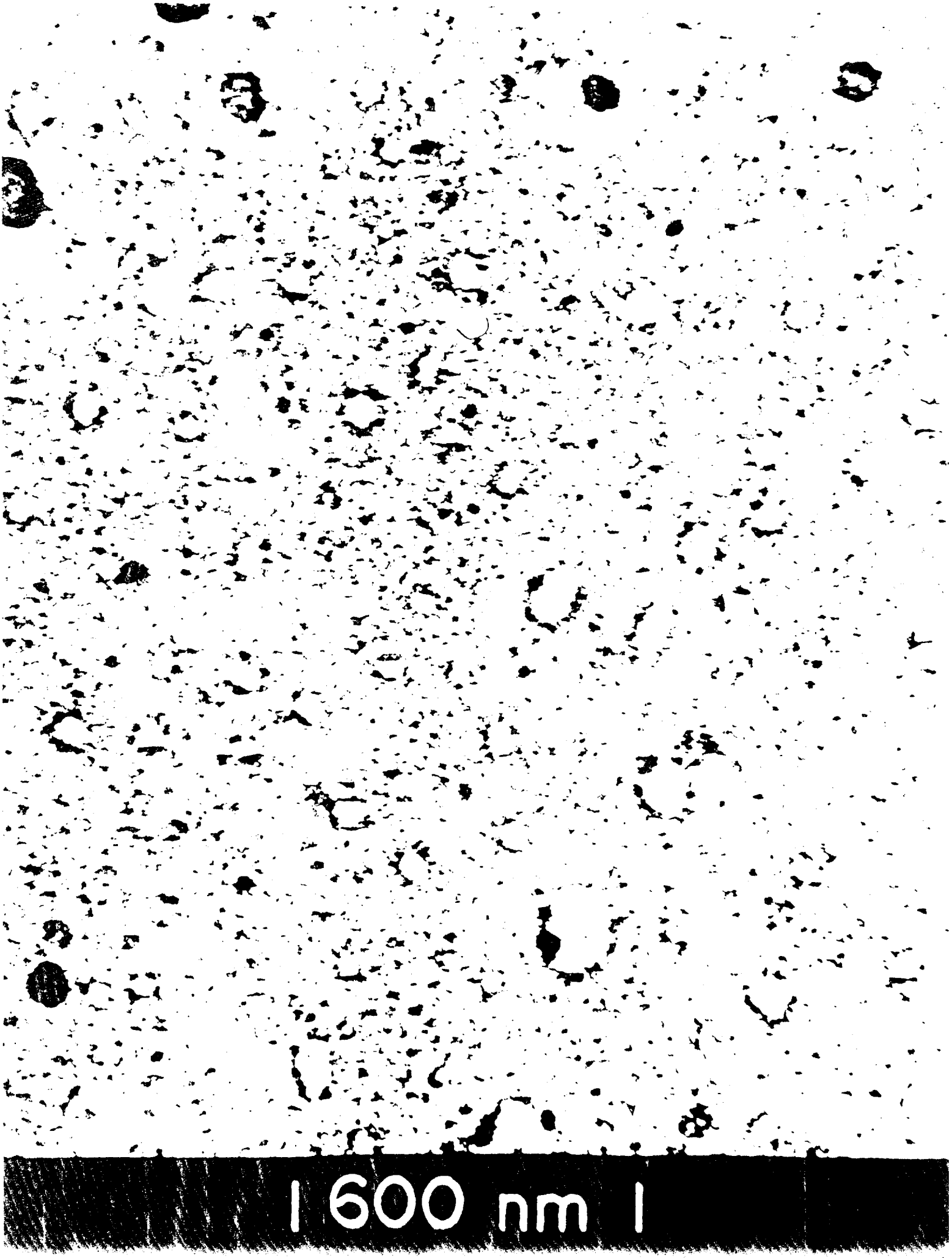
1 600 nm 1


Ru
6.5 μm

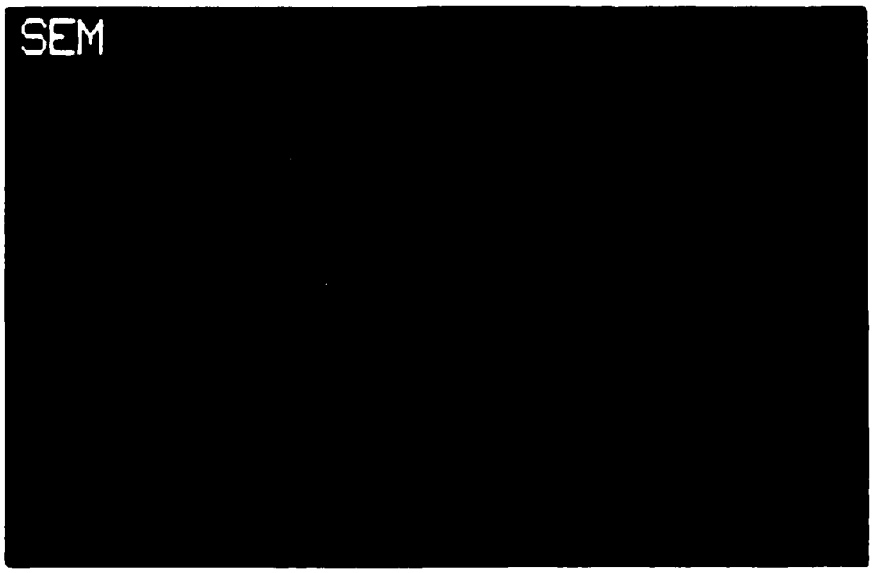
SEM

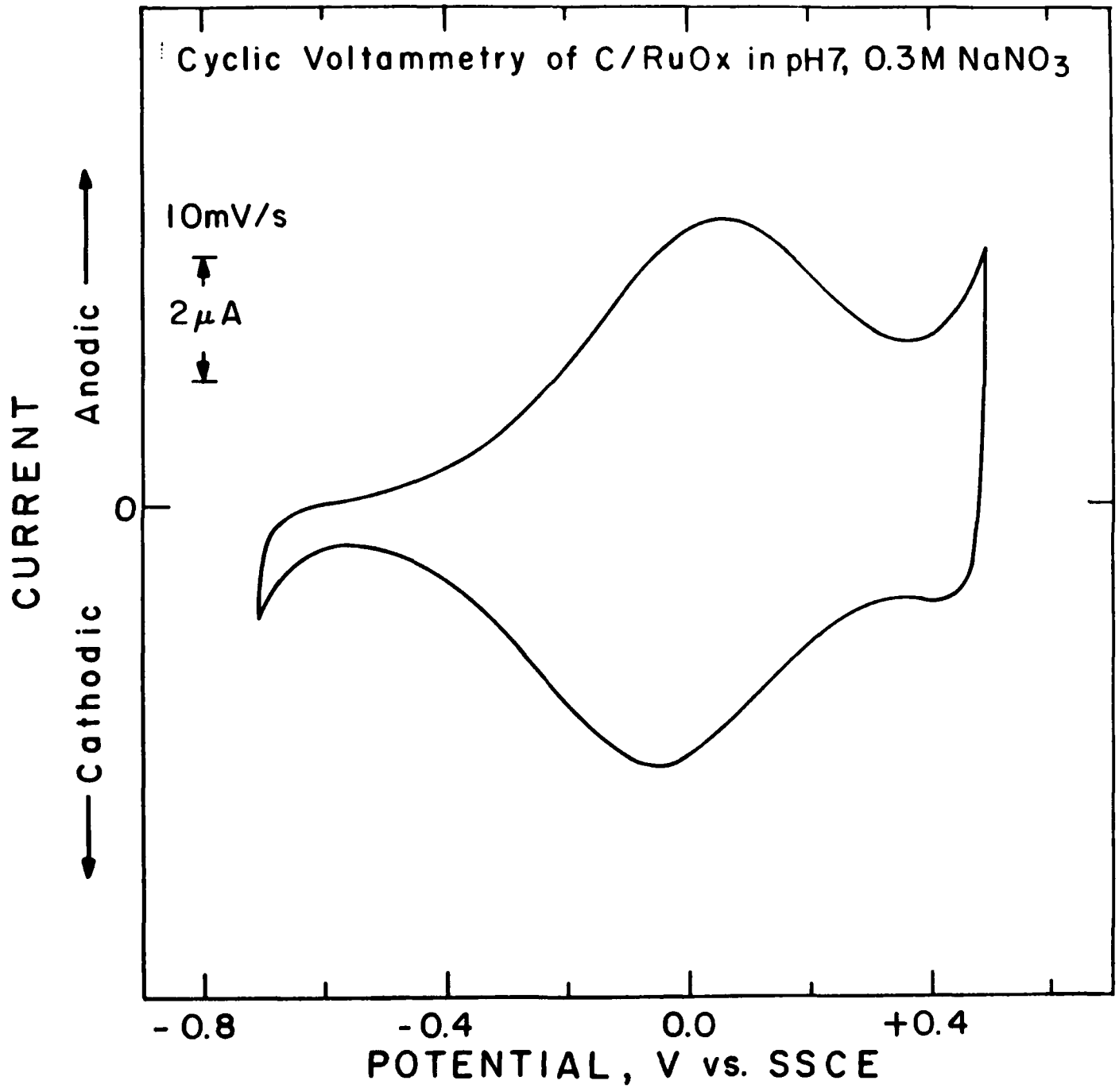
Cyclic Voltammetry of C/RuOx in pH7, 0.3M NaNO3
10mV/s
2μA
CURRENT
Anodic
Cathodic
0
-0.8
-0.4
0.0
+0.4
POTENTIAL, V vs. SSCE

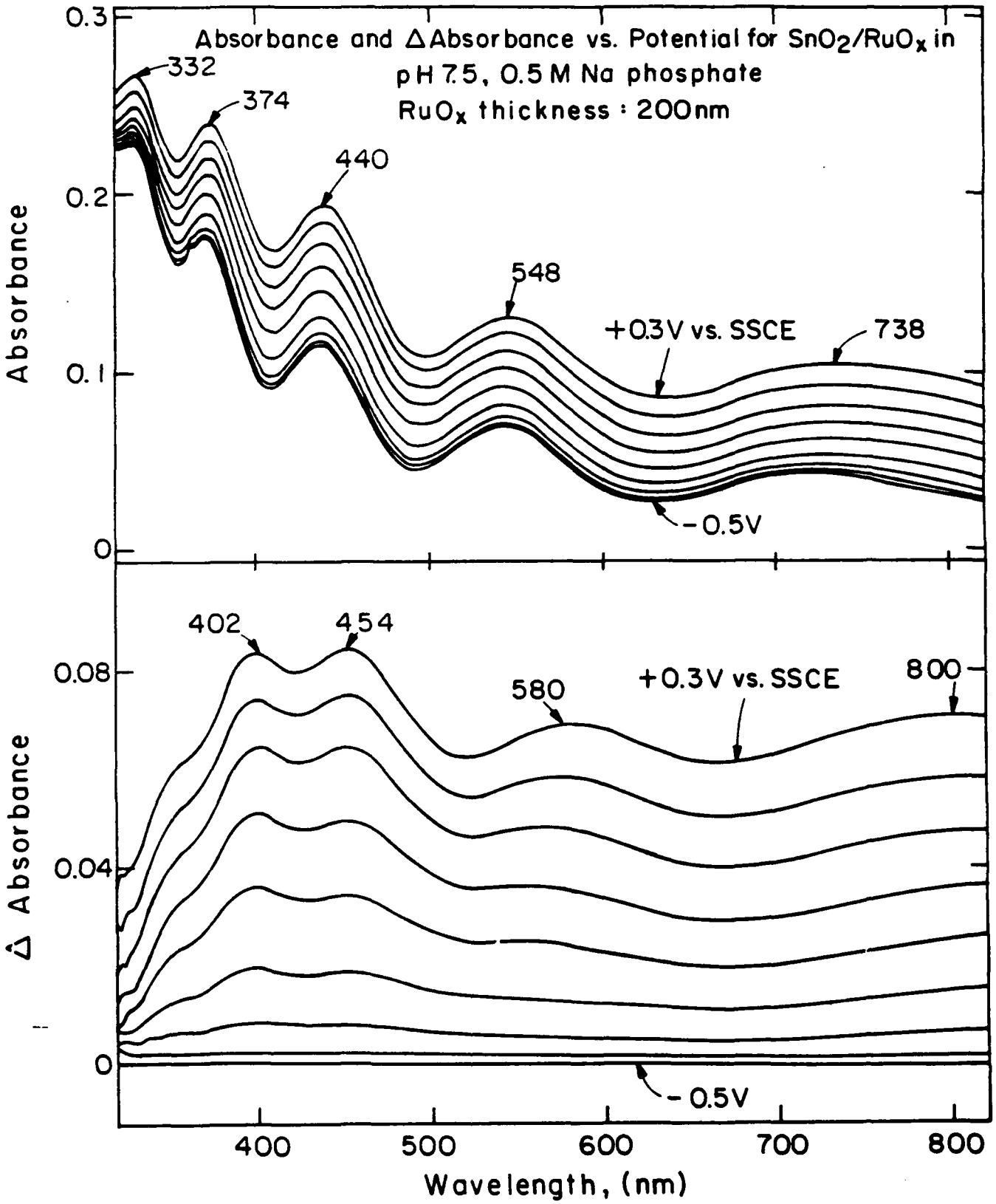
Absorbance and ΔAbsorbance vs. Potential for SnO2/RuOx in
pH 7.5, 0.5 M Na phosphate
RuOx thickness : 200nm
332
374
440
548
+0.3V vs. SSCE
738
-0.5V
Absorbance
0.3
0.2
0.1
0
402
454
580
+0.3V vs. SSCE
800
-0.5V
Δ Absorbance
0.08
0.04
0
400
500
600
700
800
Wavelength, (nm)

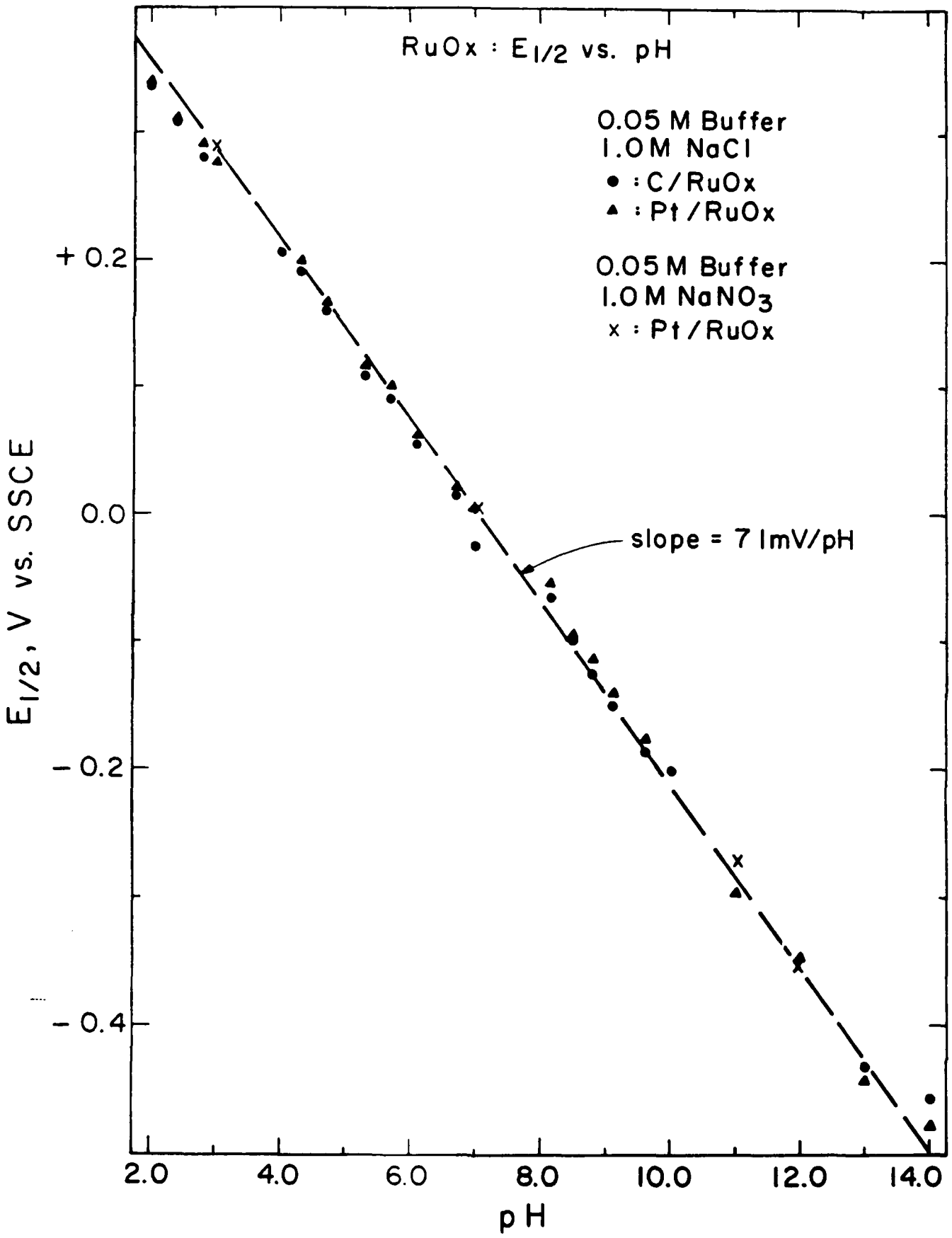
RuOx : E1/2 vs. pH
0.05 M Buffer
1.0 M NaCl
● : C/RuOx
▲ : Pt/RuOx
0.05 M Buffer
1.0 M NaNO3
x : Pt/RuOx
slope = 71 mV/pH
+0.2
0.0
−0.2
−0.4
E1/2, V vs. SSCE
2.0
4.0
6.0
8.0
10.0
12.0
14.0
pH

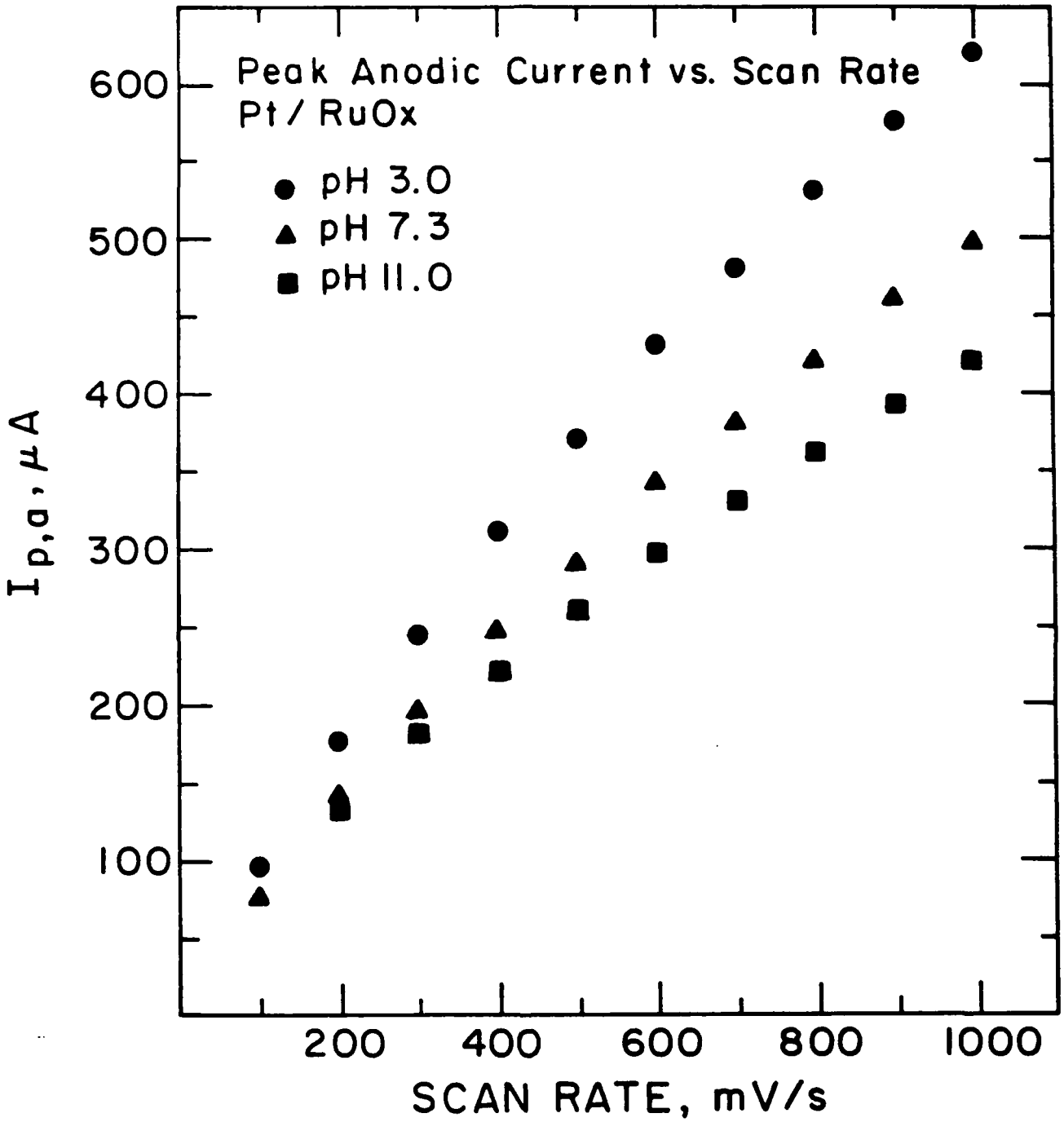
Peak Anodic Current vs. Scan Rate
Pt / RuOx
pH 3.0
pH 7.3
pH 11.0
600
500
400
300
200
100
$I_{p,a}$, μA
200
400
600
800
1000
SCAN RATE, mV/s

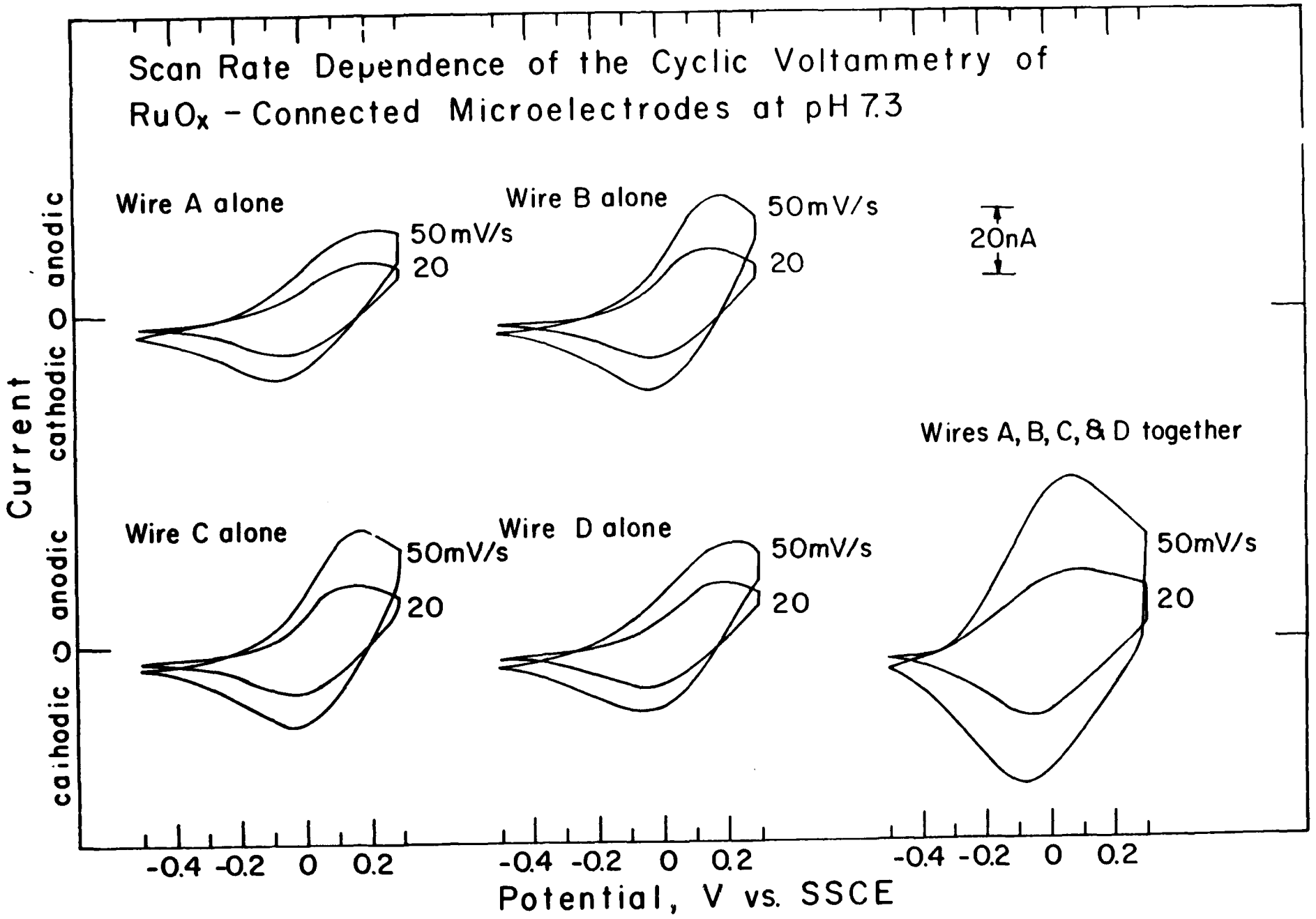
Scan Rate Dependence of the Cyclic Voltammetry of
RuOx - Connected Microelectrodes at pH 7.3
Wire A alone
50mV/s
20
Wire B alone
50mV/s
20
20nA
Wires A, B, C, & D together
50mV/s
20
Wire C alone
50mV/s
20
Wire D alone
50mV/s
20
Current
anodic
cathodic
0
anodic
cathodic
0
-0.4 -0.2 0 0.2
-0.4 -0.2 0 0.2
-0.4 -0.2 0 0.2
Potential, V vs. SSCE

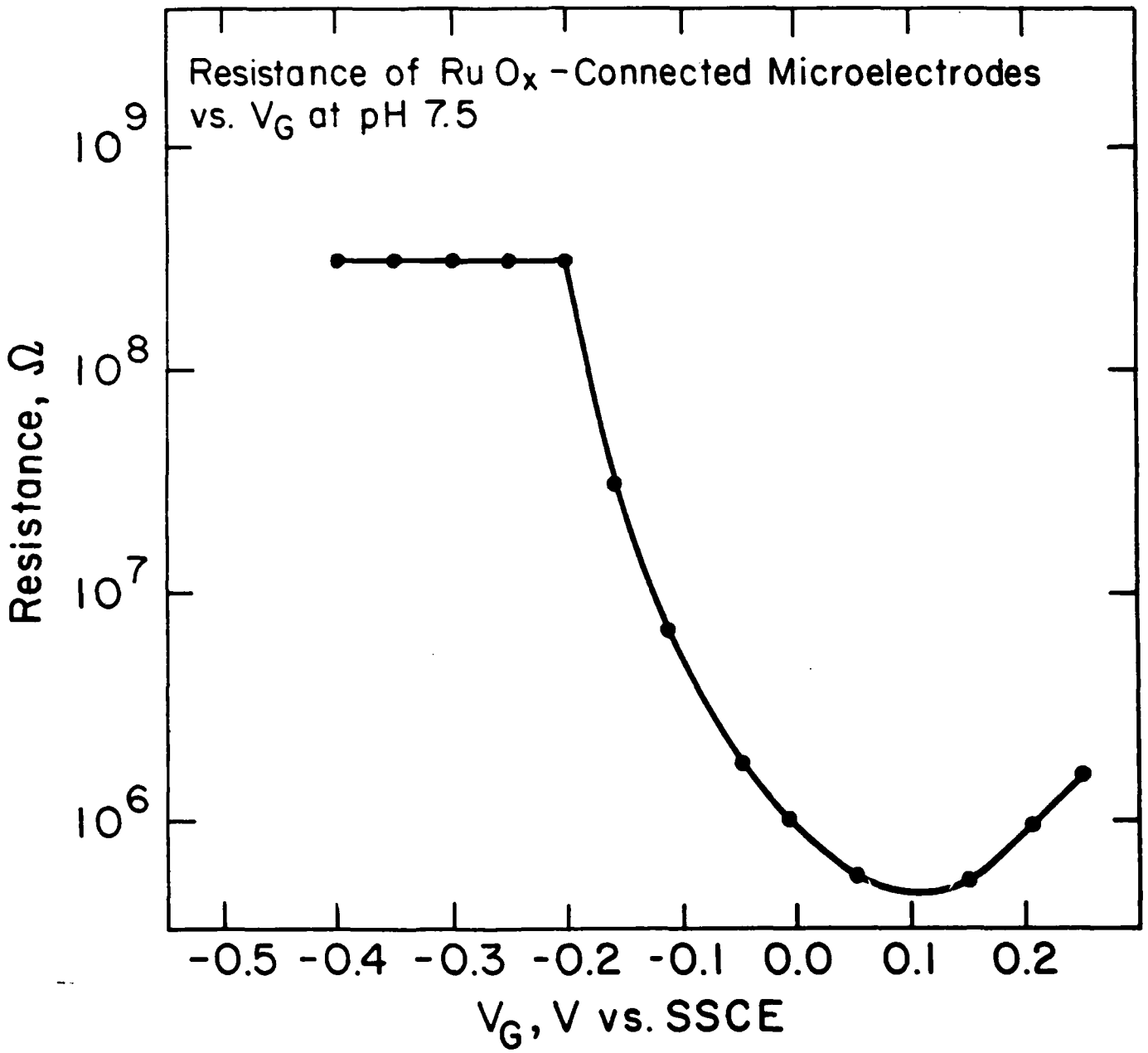
Resistance of Ru Ox -Connected Microelectrodes
vs. VG at pH 7.5
Resistance, Ω
10^9
10^8
10^7
10^6
-0.5 -0.4 -0.3 -0.2 -0.1 0.0 0.1 0.2
VG, V vs. SSCE

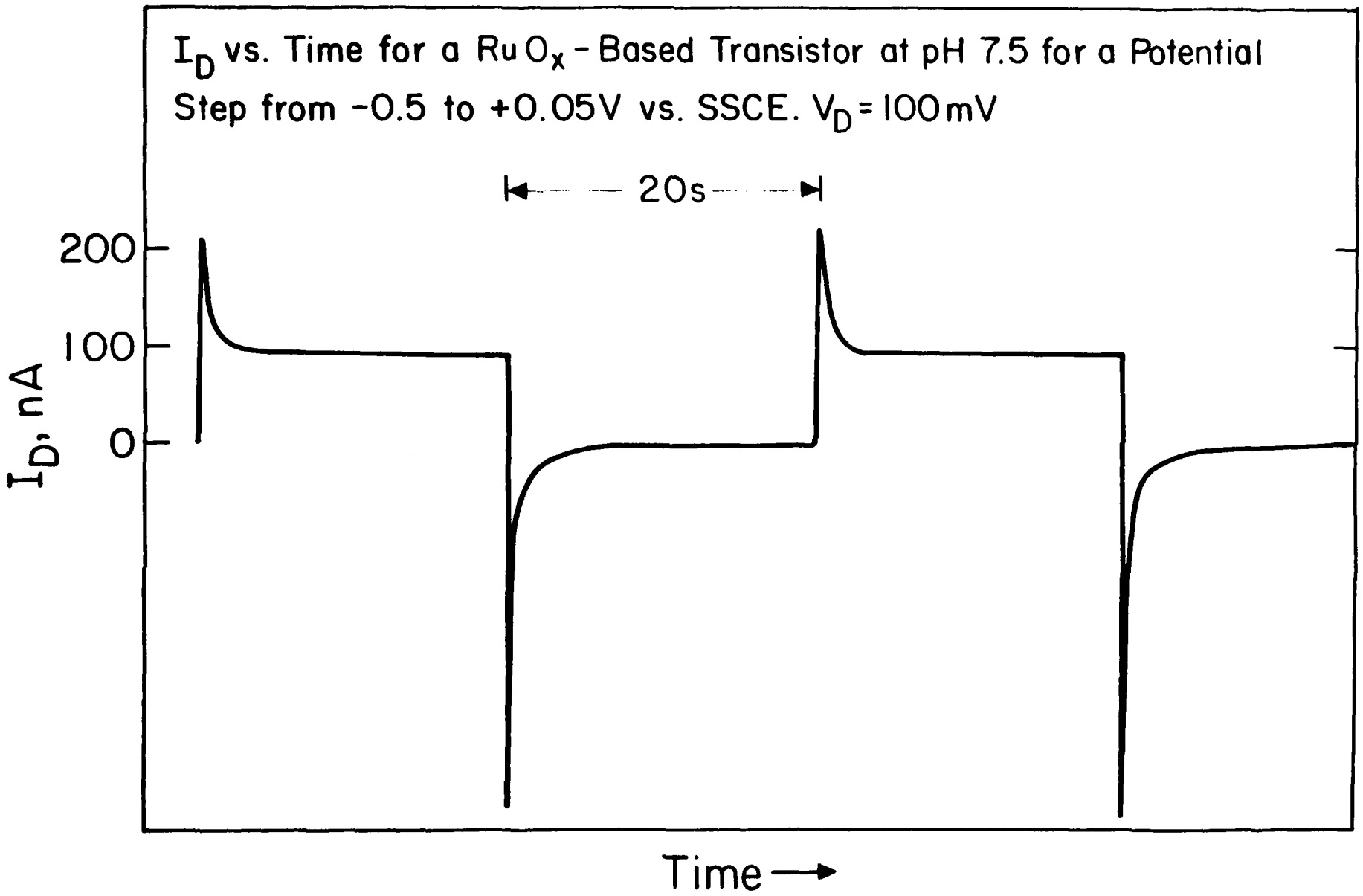
I_D vs. Time for a RuO_x - Based Transistor at pH 7.5 for a Potential Step from -0.5 to +0.05V vs. SSCE. V_D = 100 mV
20s
200
100
0
I_D, nA
Time

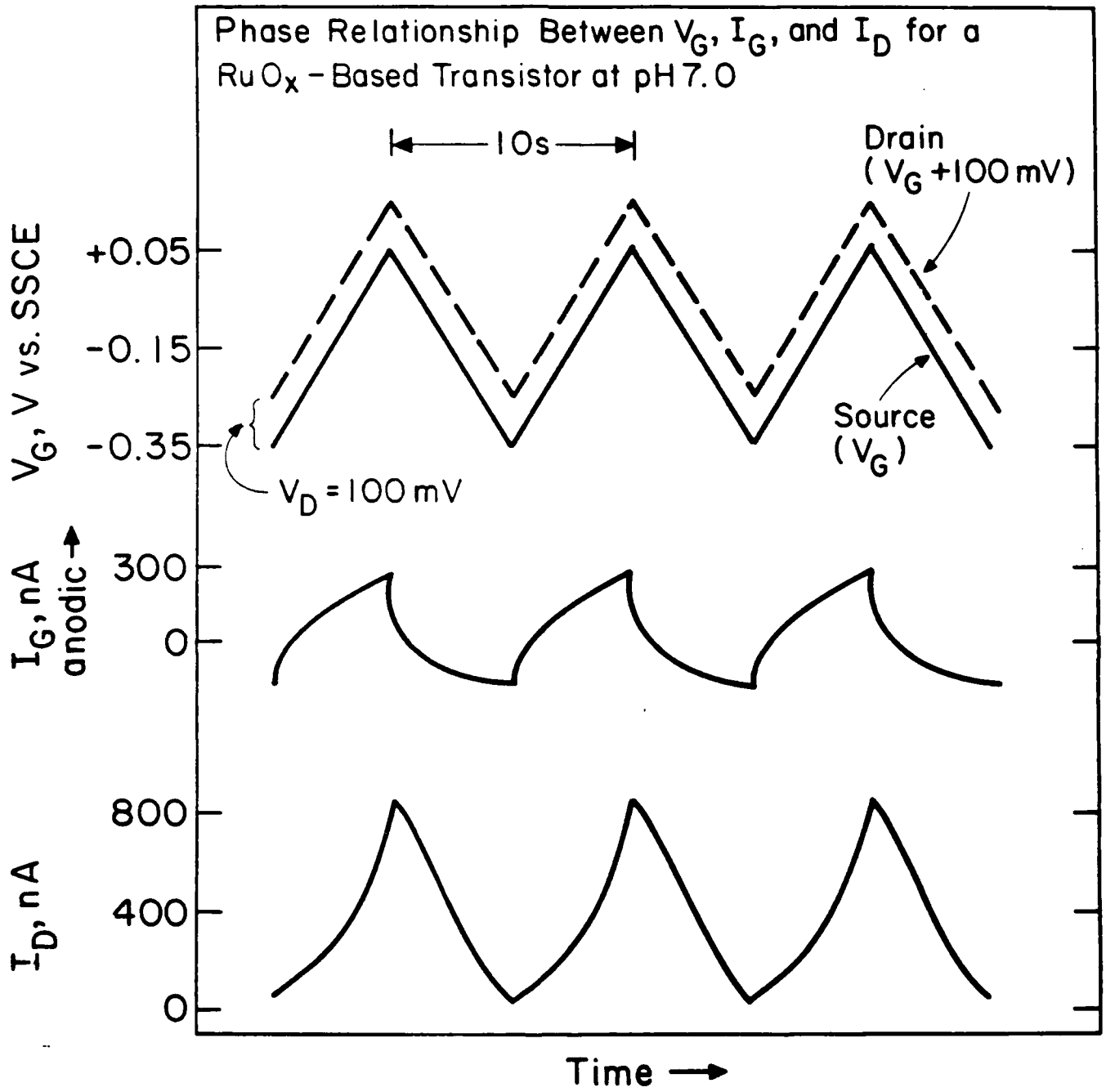
Phase Relationship Between V_G, I_G, and I_D for a
RuO_x - Based Transistor at pH 7.0
10s
Drain
(V_G +100 mV)
Source
(V_G)
V_D = 100 mV
V_G, V vs. SSCE
+0.05
-0.15
-0.35
I_G, nA
anodic
300
0
I_D, nA
800
400
0
Time

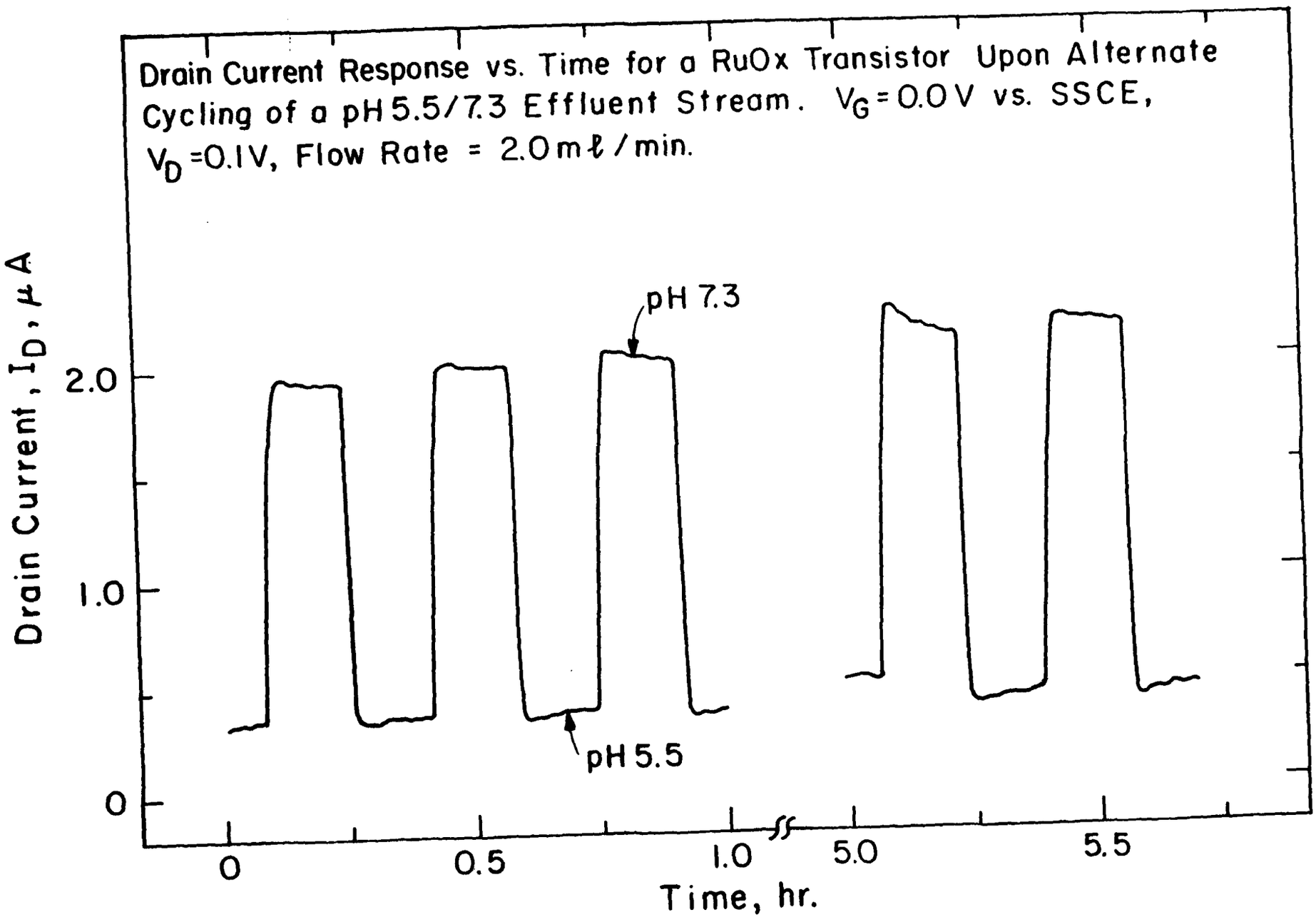
Drain Current Response vs. Time for a RuOx Transistor Upon Alternate Cycling of a pH 5.5/7.3 Effluent Stream. V_G = 0.0 V vs. SSCE, V_D = 0.1 V, Flow Rate = 2.0 mℓ/min.
pH 7.3
pH 5.5
Drain Current, I_D, μA
2.0
1.0
0
0
0.5
1.0
5.0
5.5
Time, hr.

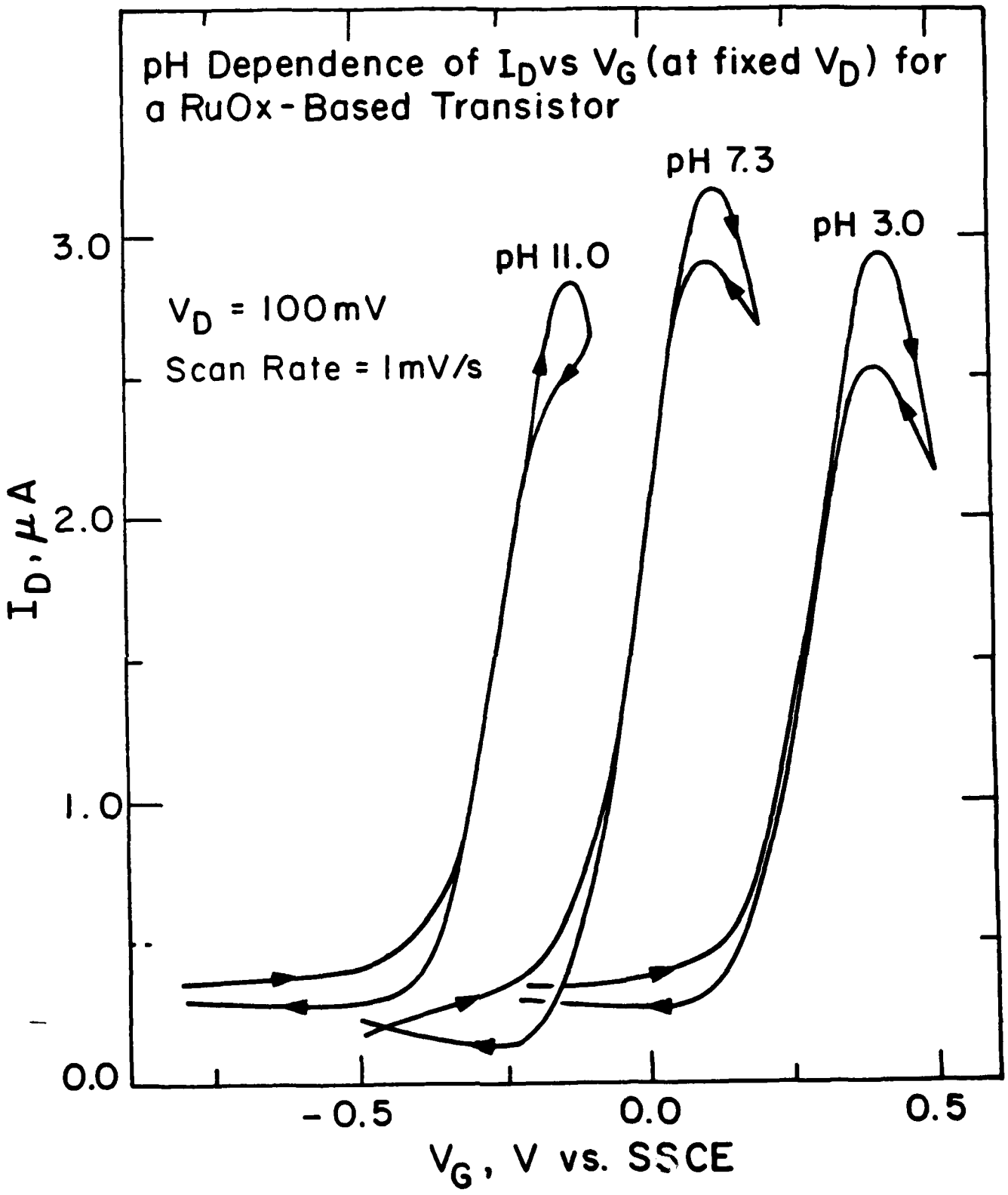
pH Dependence of I_D vs V_G (at fixed V_D) for a RuOx-Based Transistor
pH 7.3
pH 3.0
pH 11.0
V_D = 100mV
Scan Rate = 1mV/s
3.0
2.0
1.0
0.0
I_D, μA
-0.5
0.0
0.5
V_G, V vs. SSCE